The Microbe 5 (2024) 100186

Contents lists available at ScienceDirect

The Microbe

journal homepage: www.sciencedirect.com/journal/the-microbe

Pathogenicity of psychrotolerant strains of Antarctic *Pseudogmynoascus* fungi reveals potential opportunistic profiles

Eldon Carlos Queres Gomes [a], Vívian Nicolau Gonçalves [a], Marliete Carvalho da Costa [a], Gustavo José Cota de Freitas [a], Daniel Assis Santos [a], Susana Johann [a], Jefferson Bruno Soares Oliveira [b], Tatiane Alves da Paixão [b], Peter Convey [c,d,e], Luiz Henrique Rosa [a,*]

[a] Departamento de Microbiologia, Universidade Federal de Minas Gerais, Belo Horizonte, MG, Brazil
[b] Departamento de Patologia Geral, Universidade Federal de Minas Gerais, Belo Horizonte, MG, Brazil
[c] British Antarctic Survey, NERC, High Cross, Madingley Road, Cambridge CB3 0ET, United Kingdom
[d] Department of Zoology, University of Johannesburg, PO Box 524, Auckland Park 2006, South Africa
[e] Biodiversity of Antarctic and Sub-Antarctic Ecosystems, Santiago, Chile

ARTICLE INFO

Keywords:
Climate change
Extremophiles
Fungi
Opportunistic
Virulence

ABSTRACT

Recent studies have demonstrated the presence of fungal taxa in the extreme ecosystems of Antarctica that are known to opportunistically infect humans and animals. Among these are members of the genus *Pseudogymnoascus*, including some that are genetically similar to *P. destructans*, known to be pathogenic to bats. We evaluated the *in vitro* and *in vivo* pathogenic potential of 11 *Pseudogymnoascus* spp. strains recovered from Antarctica. All strains were able to grow at temperatures up to 28 °C and displayed *in vitro* pathogenicity through hemolytic activity, growth at different pH levels, production of hydrolytic enzymes, spore diameters, tolerance to oxidative stress, hypoxia, and halotolerance. Among them, *Pseudogymnoascus* sp. UFMG 8532 exhibited strong *in vitro* pathogenicity and in preliminary *in vivo* assay killed 100 % of *Tenebrio molitor* larvae within one day. The pathogenicity of the same strain was also tested using immunosuppressed BALB/c mouse models. Survival of BALB/c mice was affected, with oscillations between weight gain and loss, and impacts on sensory function, reflexes and autonomic function. Histopathological data from the organs of infected mice showed evidence of inflammatory processes, with numerous neutrophils, a small number of macrophages, fluid accumulation inside the lungs and intense hyperemia. Our results indicate that Antarctic *Pseudogymnoascus* spp. strains obtained from various substrates/habitats in maritime Antarctica may possess intrinsic virulence factors and pathogenic potential for immunosuppressed animals and humans in the region. Given that the Antarctic environment is an important reservoir for *Pseudogymnoascus* species, which display growth performance across a range of temperatures, it is possible that increasing temperatures in the maritime Antarctic could activate dormant genes or biochemical pathways, select virulent species and/or strains, and facilitate their spread within and beyond the region. The ability of *Pseudogymnoascus* species to grow slowly even at 28°C, coupled with their potential *in vitro* and *in vivo* virulence factors, suggests that these fungi might be undergoing an opportunistic transition due to the effects of climate change on the Antarctic Peninsula.

1. Introduction

Antarctica is characterized by environmental conditions that limit the survival of terrestrial animals and plants; however, microorganisms are able to thrive in its various ecosystems (Ruisi et al., 2007). Resident microorganisms represent the largest component of biodiversity in terrestrial Antarctica and may possess unique genetic and biochemical characteristics (Onofri, 1999; Arenz et al., 2014; Rosa et al., 2019). Amongst Antarctic microorganisms, research on fungi ranges from systematics to biotechnological applications, and recognises their

* Correspondence to: Laboratório de Microbiologia Polar e Conexões Tropicais, Departamento de Microbiologia, Instituto de Ciências Biológicas, Universidade Federal de Minas Gerais, Belo Horizonte, PO Box 486, MG CEP 31270-901, Brazil.
E-mail address: lhrosa@icb.ufmg.br (L.H. Rosa).

https://doi.org/10.1016/j.microb.2024.100186
Received 14 March 2024; Received in revised form 4 October 2024; Accepted 7 October 2024
Available online 9 October 2024

interactions with humans, animals and plants (Rosa et al., 2019).

Global diversity of fungi is high, but only a small proportion of this diversity (around 400 species) is reported to be pathogenic towards humans (Parrish and Riedel, 2014). The factors that determine the pathogenicity of a microorganism can be investigated through various approaches, such as the evaluation of hemolytic activity, thermotolerance, production of hydrolytic enzymes, influence of pH on growth, spore morphology, and their capacity for morpho-physiological dimorphism (Casadevall, 2012). Some studies have reported the isolation of fungal species with pathogenic potential for humans, animals and plants from substrates collected in Antarctica (Alves et al., 2019; de Sousa et al., 2017; Gonçalves et al., 2017; Rosa et al., 2020a; Figueredo et al., 2020). However, little is yet known about the magnitude of risk posed by opportunistically pathogenic fungal taxa present in different Antarctic habitats.

The largest component of fungal diversity present in Antarctica are cosmopolitan genera adapted to cold and stressful conditions, with a small proportion of taxa currently recognized as endemic (Rosa et al., 2019). Amongst these, the Ascomycota genus *Pseudogymnoascus* (previously classified as *Geomyces*) currently includes 25 described species globally (www.mycobank.org), of which 19 have currently been reported in Antarctica (Villanueva et al., 2021). *Pseudogymnoascus* species appear to have the ability to colonize multiple habitats and utilize different carbon sources and can be abundant in low temperature ecosystems (Arenz and Blanchette, 2011). This genus has been reported across Arctic, alpine and temperate regions, and Antarctica (Mercantini et al., 1989; Onofri, 1999; Zukal et al., 2016).

Some studies in Antarctica have reported lineages identified as *Pseudogymnoascus* sp. with high genetic similarity with *P. destructans* (Li et al., 2008; Brunati et al., 2009; Tsuji et al., 2013; Edgington et al., 2014; Furbino et al., 2014; Chávez et al., 2015; Figueroa et al., 2015; Godinho et al., 2015; Gonçalves et al., 2015; Santiago et al., 2015; Connell et al., 2018; Purić et al., 2018; Alves et al., 2019). Amongst the members of *Pseudogymnoascus*, *P. destructans* is known for being pathogenic and responsible for reducing bat populations through White-Nose Syndrome (Blehert et al., 2009; Gargas et al., 2009; Lorch et al., 2011). Bats infected with *P. destructans* may exhibit visible fungal growth on their snout and wing membranes, awaken early from hibernation (Blehert, 2012; Fisher et al., 2012), and experience premature depletion of fat reserves, leading to death within 70–120 days post-infection (Hoyt et al., 2015). Bats in caves in North America and Europe are often infected by *P. destructans*, conidia being dispersed when they exit hibernation early (Lorch et al., 2011). The spores can then infect other bats in the environment (Wilson et al., 2017) and colonize various substrates (Raudabaugh and Miller, 2013).

Limited knowledge of the pathogenicity of native Antarctic fungi, combined with the presence of *Pseudogymnoascus* taxa genetically similar to *P. destructans*, are significant stimuli for evaluating the pathogenic potential of strains obtained from various substrates in Antarctica. The objective of our study was to evaluate the pathogenicity of different strains of *Pseudogymnoascus* spp. obtained from Antarctica through *in vitro* and *in vivo* assays, thereby contributing to the recognition of any risks potentially posed by these cold-adapted fungi that can be present in high abundance in various parts of maritime Antarctica.

2. Material and methods

2.1. Antarctic Pseudogymnoascus spp. strains

The 11 *Pseudogymnoascus* spp. strains used in this study were originally isolated from various lichen thalli and soils obtained on the South Shetland Islands, maritime Antarctica (Suppl. Table 1), which were genetically similar to the pathogenic species *P. destructans* based on ITS BLAST analysis. For the current study, they were obtained from the Collection of Microorganisms and Cells of the Universidade Federal de Minas Gerais, Brazil.

2.2. In vitro pathogenicity assays

2.2.1. Thermotolerance and growth

The 11 strains were inoculated by transferring 4 mm^2 blocks from 10-day-old pre-cultures grown at 15 °C on YM (0.3 % yeast extract, 0.3 % malt extract, 0.5 % peptone, 2 % glucose, 2 % agar) at 5, 10, 15, 20, 25, 28, 30 and 37 °C using Petri dishes (90 ×15 mm) and incubated for 3, 7, 14 and 21 d in triplicate for each strain. Colony diameter was then measured in millimeters. Data obtained were subjected to analysis of variance and, when significant, pairwise differences between means were assessed using the least significant difference test (LSD) with P = 0.05.

2.2.2. Influence of pH on growth

The fungal strains were grown in triplicate in Petri dishes (90 × 15 mm) on YM agar adjusted to pH 4 (mammalian vaginal pH), pH 7 (tissue and blood pH), and pH 9 (intestinal pH) at 28 °C for 7 d, as described by Davis (2009). Growth was then assessed.

2.2.3. In vitro pathogenic assay

The fungal inoculum was obtained as described above. Hemolytic

Table 1
Characterization of *in vitro* pathogenicity of the 11 Antarctic *Pseudogymnoascus* spp. strains studied.

	Hemolytic activity		Growth at 28 °C in different pH			Production of hydrolytic enzymes (halo in mm)							
UFMGCB code[a]	Hi[b]	H[c]	pH 4	pH 7	pH 9	Pho[e] (Pz)[g]	Pro[e] (Pz)[g]	Est[g] (Pz)	Ure[k]	Spores measures (μm)	Ost[o]	Hyp[p]	Hal[q]
8532	0.99	γ[d]	+	+	+	0.60	-[h]	0.72	++[l]	2.68 ± 0.48 ×3.50 ± 0.61	-[i]	-	-[i]
8562	0.99	γ	+[f]	+	+	0.23	-	0.75	++	2.55 ± 0.80 ×2.95 ± 0.80	-	+[f]	+[f]
10326	0.50	α[e]	+	+	+	0.99	-	0.67	-	2.39 ± 0.44 ×3.08 ± 0.55	-	-	-
10378	0.52	α	+	+	+	0.20	-	0.71	++	2.61 ± 0.38 ×3.86 ± 0.43	-	+	+
10381	0.70	α	+	+	+	0.35	-	0.70	++	2.38 ± 0.31 ×3.38 ± 0.62	-	+	+
10386	0.68	α	+	+	+	0.51	-	0.73	+-[m]	2.13 ± 0.51 ×3.28 ± 0.74	-	+	+
10392	0.74	α	+	+	+	0.30	-	0.72	+[n]	2.36 ± 0.43 ×3.42 ± 0.60	-	+	+
10394	0.57	α	+	+	+	0.54	-	0.90	+-	3.20 ± 0.79 ×3.98 ± 1.33	-	-	-
10472	0.37	α	+	+	+	0.55	-	ND[i]	-	2.16 ± 0.44 ×2.57 ± 0.65	-	-	-
10479	0.71	α	+	+	+	0.16	-	ND	-	2.59 ± 0.41 ×3.30 ± 0.42	-	+-	+
10504	0.48	α	+	+	+	0.32	-	0.99	+	2.22 ± 0.44 ×2.93 ± 0.56	-	-	-

[a] UFMGCB = Collection of Micro-organisms and Cells of the Universidade Federal de Minas Gerais.[b]Hi = Hemolytic index and [c]H = Type of hemolysis: [d]γ = Gamma (absent) and [e]α = Alpha (partial), [f](+) = growth. [d]Pho = Phospholipase activity. [e]Pro = proteinase activiy and [f]Est = esterase activity [g]Pz = Proteolytic enzymatic activity: strong positive (Pz ≤ 0.69 mm), strong (Pz between 0.70 and 0.79 mm), medium (Pz between 0 and 80–0–89 mm), weak (Pz between 0.90 and 0.99 mm).] [h](-) = absence of growth and [i]ND = not detected. [k]Ure = Urease activity; [l](++) = strong positive, [m](+-) = positive and [n](+) = weak positive. [o]Ost = Oxidative stress tolerance, [p]Hip = Hypoxia and [q]Hal = Halotolerance.

activity was determined on sheep blood agar following Schaufuss et al. (2007). Petri dishes were incubated at 28°C for 7 d. The hemolytic index (H) was assessed visually by the presence of a halo around the colony. A transparent halo indicates beta hemolysis (complete), a greenish halo indicates alpha hemolysis (partial), and the absence of a halo indicates gamma hemolysis (absent).

2.2.4. Production of hydrolytic enzymes

All fungal strains were assessed using phospholipase and proteinase assays, following Price et al. (1982) and Aoki et al. (1990), respectively. For phospholipase activity, the medium included sodium chloride (5.73 %), calcium chloride (0.05 %) and Sabouraud agar (2 %). The medium was autoclaved and then cooled to approximately 40 °C before the addition of sterile egg yolk to a final concentration of 4 %. The plates were incubated at 28 °C for up to 7 d. Precipitation around the colonies indicated phospholipase production. For esterase activity, the isolates were cultivated in a medium composed of $CaCl_2H_2O$ (4 g L^{-1}), NaCl (5 g L^{-1}), peptone (10 g L^{-1}), Tween 80 (10 g L^{-1}) and agar (20 g L^{-1}), and the presence of a white precipitate around the colony confirmed enzyme production (Martorell et al., 2017). *Candida albicans* ATCC 10231 was used as the positive control and the assessments were performed in triplicate.

For the proteinase activity the fungal isolates were inoculated on ASB agar (11.7 % yeast carbon base, 1 % yeast extract, 2 % bovine serum albumin, 2 % agar, pH 5) and incubated for 7 d at 28 °C. Proteinase activity was assessed using the halo size of the hydrolysis opacity of ASB. The proteolytic enzymatic activity (Pz) was calculated based on the ratio between the diameter of the colony and the diameter of the degradation zone of the substrate and classified as very strong (Pz $\leq$ 0.69), strong (Pz between 0.70 and 0.79), normal (Pz between 0.80 and 0.89) or weak (Pz between 0.90–0.99). Assessment of urease activity followed the protocol of Christensen, (1946). Briefly, the fungal strains were inoculated at 28 °C for 7 or 14 d in Christensen agar. Urease production was indicated by a dark pink color, while the negative result was indicated by unchanged color.

2.2.5. Spore size and polymorphism capability

All fungal strains were grown on Petri dishes containing CMA medium for spore size determination. The cultures were then mounted on slides in methylene blue prepared in polyvinyl-lactophenol and 75 spores were measured microscopically (Leica DM750, Germany).

2.2.6. Antifungal susceptibility

The minimum inhibitory concentrations (MICs) of the 11 *Pseudogymnoascus* spp. strains were determined on exposure to the antifungal drugs itraconazole, fluconazole and amphotericin B (both Sigma, USA). The MIC protocol was performed using a modified version of the method used for filamentous fungi (CLSI, 2008) in RPMI-1640 medium (INLAB, Brazil). The fungal isolates were previously grown in CMA medium at 7 °C for 16 d and the colonies were covered with sterilized saline solution (0.85 % NaCl). The liquid containing the spores was then transferred to a sterilized test tube and, after sedimentation by decantation, the supernatant was transferred to another sterilized test tube and vortexed for approximately 15 sec. The spores were counted using a Neubauer camera and a standardized solution of 10^6 spores mL^{-1} was prepared. Assays were carried out using 96-well microtiter plates. The fungal spore suspensions were treated with itraconazole (0.015–16 μg mL^{-1}), fluconazole (0.062–64 μg mL^{-1}) or amphotericin B (from 0.007 to 8 μg mL^{-1}). Microtiter plates containing spores were incubated at 28 °C for 7 d. All MIC assays were performed in duplicate.

2.2.7. Oxidative stress tolerance

Oxidative stress tolerance was determined as described by Cunha et al. (2010). Briefly, H_2O_2 (Merck, USA) was added directly to control and treated cultures to final concentrations of 0.005, 0.05 and 0.5 M. Conidia (2×10^8 cells mL^{-1}) were incubated in RPMI-1640. From each sample, 50 μL was placed in wells of a 24-well plate with 500 μL of 3 % Czapek Dox agar (Difco, USA). Cultures were incubated at 28 °C for 7 d. Assays were performed in duplicate and results were evaluated by the absence or presence of mycelial growth.

2.2.8. Hypoxia determination

Fungal isolates were inoculated in YM medium and incubated in a microaerophilia jar at 28 °C for 7 d (Grahl et al., 2011). Tests were carried out in duplicate and fungal isolates that showed growth under these conditions were considered a positive result.

2.2.9. Halotolerance

Halotolerance was determined as described by Evans et al. (2013). Five millimeters of fungal mycelial growth were inoculated onto the center of YM agar Petri dishes supplemented with 2 % NaCl. Plates were grown at 28 °C for 7 d. Assays were performed in duplicate and fungal isolates that showed mycelial growth were considered positive.

2.2.10. Fungal taxonomy

The 11 strains were subjected to genetic and morphological taxonomic study. DNA extraction was carried out as described by Rosa et al. (2009) and the internal transcribed spacer (ITS) region was amplified using the universal primers ITS1 and ITS4 (White et al., 1990). To achieve species-rank identification based on ITS data, the consensus sequence was aligned with all sequences from related species retrieved from the NCBI GenBank database using BLAST (Altschul et al., 1997). A phylogenetic tree constructed using the maximum composite likelihood method was employed to estimate evolutionary distances, with bootstrap values calculated from 1000 replicate runs using the program MEGA 11 (Tamura et al., 2021).

For morphological identification, slides were mounted on microculture plates and incubated at 15 °C for 28 d on Sabouraud agar (SBA - Kasvi, Brazil) as described by Villanueva et al. (2021). The prepared slides were fixed in 95 % ethanol and stained with lactophenol blue/-cotton blue for subsequent photographic recording of the reproductive structures using an image capture system (Leica DFC425, USA).

2.3. In vivo assays

2.3.1. Preliminary in vivo pathogenic assay using the host invertebrate model Tenebrio molitor

The *Pseudogymnoascus* spp. strains. were cultivated in CMA for 16 d at 15 °C before testing. For experiments, spores were suspended in phosphate-buffered saline (PBS) and counted in a Neubauer chamber. The concentration of viable conidia was obtained after staining with Trypan Blue.

The assay model used larvae of the invertebrate *Tenebrio molitor* following the protocol of da Silva et al. (2018). Briefly. *T. molitor* beetle larvae were commercially obtained (Senhor Tenebrios Company, Brazil) and maintained in our laboratory. To perform survival analyses, larvae of 0.1–0.2 g mass without signs of contamination spots or exoskeleton changes were selected. Each larva, after brief surface cleaning with 70 % ethanol, was infected directly in the hemocele using a Hamilton syringe (701 N, caliber 26, 10 μL capacity). Spores at 10^8 of *Pseudogymnoascus* sp. UFMGCB 8532 were injected into each *T. molitor* larva. Each experimental group consisted of 10 larvae, using uninfected larvae with 5 mL of phosphate buffered saline (PBS) (negative control), infected larvae, with the target fungi and/or larvae infected with *C. albicans* SC5314 (control). Infected larvae and negative controls were incubated in Petri dishes at 37 °C and their viability was examined at 24 h intervals over 10 d. The larvae were considered dead if they did not respond to mechanical stimulus. Survival curves were plotted and statistical analyses were performed using the Log-rank (ManteleCox) test with Graph Pad Prism software and were considered statistically significant at $P < 0.05$.

2.3.2. Ethics statement for in vivo mice assay

Female BALB/c mice (n = 6 mice per group), six-to-eight weeks old, were obtained from the Universidade Federal de Minas Gerais for use in *in vivo* experiments. Water and food were provided *ad libitum*, and mice were kept in rooms with 12 h/12 h light/dark cycles. We followed the Brazilian Society of Zootechnics/Brazilian College of Animal Experimentation guidelines (available at http://www.cobea.org.br/) and Federal Law 11794. These were approved by the Ethics Committee on Animal Use of the Universidade Federal de Minas Gerais (CEUA/UFMG, protocol nº 313/2016). The animals were anesthetized intraperitoneally with ketamine (80 mg kg^{-1}) (Cetamin® Syntec, SP, Brazil) and xylazine (15 mg kg^{-1}) (Xilazin® Syntec, SP, Brazil) before experimentation. All experimental procedures were carried out according to the standards of the Brazilian Society of Laboratory Animal Science/Brazilian College for Animal Experimentation (available at http://www.sbcal.org.br).

2.3.3. In vivo assay against immunocompromised BALB/c mice

To obtain the spores used in this experiment, the selected strain *Pseudogymnoascus* sp. UFMGCB 8532 was cultivated on CMA agar and incubated at 7 °C for 16 d. The spore inocula were prepared as described by Santos and Hamdan (2005). The *in vivo* assays were performed with female BALB/c mice, six-to-eight weeks old, as described by Ferreira et al. (2015). Further groups of mice were immunosuppressed using oral Dexamethasone (Decadron/Aché 10 mg/kg/day) in their drinking water for 5 d prior to the experiment (dos Santos Brito et al., 2011). Prior to intranasal infection, animals (five per group) were anesthetized by intraperitoneal (i.p.) injection with ketamine hydrochloride (ZOOSERV) (60 mg kg^{-1}) and xylazine (ZOOSERV) (10 mg kg^{-1}) in sterile saline solution (0.85 %). Inocula of 1×10^8 spores of *Pseudogymnoascus* UFMGCB 8532 were used to infect the mice. A control group was inoculated with phosphate buffered saline (PBS). The mice were monitored daily for survival and symptoms such as piloerection, hyperventilation, reduced motility and weight loss were recorded.

2.3.4. Mice survival and behavior

To examine the effects of immunosuppression in mice, dexamethasone (Decadron, Aché Laboratórios LTDA, Brazil) was administered intraperitoneally (ip) at a dose of 10 mg/kg/day, 5 days before and continuously after infection. A fungal suspension containing 1×10^8 spores 50 μL^{-1} was prepared. The suspension was inoculated intranasally. After infection, the animals were monitored daily for survival analysis and behavior assessment using the SmithKline/Harwell/ImperialCollege/RoyalHospital/Phenotype Assessment (SHIRPA) protocol (Lackner et al., 2006; Pedroso et al., 2010; Santos et al., 2014; Costa et al., 2016). The protocol provides reliable information about murine behavior. The individual parameters evaluated were grouped into five functional categories: neuropsychiatric state, motor behavior, autonomic function, muscle tone and strength, and reflex and sensory function. The score for each category was calculated as described by Oliveira et al. (2017).

2.3.5. Fungal burden

After analysis of survival and behavior, another group of mice was anesthetized and infected to evaluate the fungal burden in the brain, spleen and lungs two- and five-days post infection (d.p.i.). Animals were euthanized under anesthesia and organs were removed aseptically to quantify fungal burden. Tissues were homogenized in sterile PBS, plated on CMA and incubated at 15 °C for 7 d. Results were expressed as CFU^{-1} g.

2.3.6. Histopathology

Mouse lungs were sampled and fixed by immersion in 10 % buffered formalin for 24 h and embedded in paraffin. Four μm tissue sections were stained with hematoxylin and eosin. Information regarding the type of cells that comprised the inflammatory process as well as its extension and adjacent structures involved were described. The lesion score used was 0 (zero) absence, 1 (one) discrete, 2 (two) moderate and 3 (three) intense inflammation; absence 0 (zero) or presence 1 (one) of intralesional agents.

2.3.7. Transmigration: endothelial cell monolayers

Corning 6.5 mm Transwells with 8 μm pores (Corning, NY, USA) were coated with 3 % collagen. hCMEC/D3 cells were cultured at 37 ºC in an atmosphere of 5 % CO_2 grown to confluence in EBM2 medium as previously described (Santiago-Tirado et al., 2019). About 5×10^4 cells per cm^2 were added to the Transwell and after confluence approximately 1×10^8 spores for *Pseudogymnoascus* sp. UFMGCB 8532 in RPMI medium were added to the apical part of the chamber and then collected at the bottom for CFU measurement. Collection times of 3, 9 and 24 h were tested to evaluate the time it took for the bottom to pass through the barrier. Wells were used without adding fungal cells.

2.3.8. Statistical analyses

All statistical analyses were performed using GraphPad Prism, version 5.0, for Windows (GraphPad Software, San Diego, CA, USA) with $p < 0.05$ considered to be significant. Kaplan-Survival curves were generated and analyzed using the log rank test. The histopathology analysis measurements were analyzed by ANOVA followed, where significant, by *post hoc* Tukeys tests to compare different groups. All experiments were performed at least twice.

3. Results

3.1. Pathogenicity in vitro

All 11 *Pseudogymnoascus* spp. strains were able to grow when incubated at temperatures up to 28 °C; however, none showed mycelial growth or spore production at temperatures of 30 and 37 °C. The strains displayed different patterns regarding hemolytic activity, growth at different pH levels, production of hydrolytic enzymes, spore diameters, tolerance to oxidative stress, hypoxia, and halotolerance (Table 1). Susceptibility to antifungal agents is shown in Table 2. Four isolates grew at all concentrations of fluconazole (MIC > 64 μg mL^{-1}). The susceptibility profile to itraconazole ranged from 0.125 to 0.5 μg mL^{-1}, and for amphotericin B, the MIC was between 0.125 and 1 μg mL^{-1}.

3.2. Taxonomy of Pseudogymnoascus spp. strains

The ITS region sequences obtained from the 11 *Pseudogymnoascus* spp. strains were compared with the sequences of type species deposited in GenBank (Supplementary Table 2). They displayed different query coverages and identity percentages, as well as numbers of nucleotides in

Table 2
Minimum Inhibitory Concentration (MIC) of Antarctic *Pseudogymnoascus* spp. strains exposed to three antifungal compounds.

	MIC[b] assessed at 28 °C in a 7 days incubation (μg mL^{-1})		
UFMGCB code[a]	Itra[c]	Fluc[d]	Amp B[e]
8532	0.25	>64	0.5
8562	0.5	>64	0.125
10326	0.25	Nd	Nd
10378	0.25	16	1
10381	0.125	8	0.25
10386	0.5	0.5	0.5
10392	0.125	4	0.5
10394	0.5	>64	0.5
10472	Nd[f]	Nd	Nd
10479	0.25	>64	0.5
10504	0.25	16	0.5

[a] UFMGCB = Collection of Microorganisms and Cells of the Federal University of Minas Gerais. [b]MIC = Minimum Inhibitory Concentration. [c]Itra= itraconazole. [d]Fluc = fluconazole. [e]Amp B = anfotericina B. [f]Nd = Not determined.

comparison with three species of *Pseudogymnoascus*: *P. destructans* (eight strains), *P. roseus* (two strains), and *P. verrucosus* (one strain). For morphological characterization, the strains were cultivated on Sabouraud dextrose agar at different temperatures for up to 21 days. At all cultivation temperatures, the macromorphological characteristics of the colonies, such as the cottony mycelium having a front with a center in yellow tones and white edges, and a back in yellow tones, were observed in all isolates (Suppl. Fig. 1). Mycelial growth rates (Suppl. Table 3) showed that, for the strains *Pseudogymnoascus* sp. UFMGCB 8532 and UFMGCB 8562, colony size increased with temperature up to 20 °C, but reduced at 25 and 28 °C. Due to its significant pathogenic characteristics *in vitro* and *in vivo*, *Pseudogymnoascus* sp. UFMGCB 8532 was taxonomically categorized using ITS phylogenetic and morphological analysis.

In addition, a specific phylogenetic analysis comparing the *Pseudogymnoascus* sp. UFMGCB 8532 ITS sequence with those available in the GenBank database is shown in. Despite the genetic similarity of the *Pseudogymnoascus* sp. UFMGCB 8532 and *P. destructans*, the phylogenetic analysis revealed that the strain *Pseudogymnoascus* sp. UFMGCB 8532 is closely related to the Antarctic endemic species *P. australis* and clusters with that species, as well as with *P. griseus* and *P. laginnosus*, the latter both recently described from Antarctica by Villanueva et al. (2021). However, as *Pseudogymnoascus* sp. UFMGCB 8532 did not have any nucleotide differences with the three endemic *Pseudogymnoascus* species, it was submitted to classical morphological taxonomy classification.

Pseudogymnoascus sp. UFMGCB 8532 was grown on SBA at 15 °C for 28 days for macro- and micromorphological taxonomic analysis and comparison with those *Pseudogymnoascus* species closest in the phylogenetic analysis (*P. australis*, *P. griseus* and *P. lanuginosus*) (Suppl. Fig. 2). On SBA (Suppl. Fig. 2A and B), colonies reached 40 mm diameter after 28 days at 15 °C, and were irregular, raised, floccose, with radially and cerebriform grooves, white to yellow, margin irregular and filiform, without visible exudate, diffusible pigments absent and reverse yellow. Hyphae forming bundles with two to eight hyphae oriented in parallel, branched, septate, hyaline, smooth, 1.4–3.3 µm wide. Absence of arthroconidia chains, single aleurioconidia on fertile hyphae, sessile or stalked (Supplementary Fig. 2C). Conidiophores abundant, erect or geniculated, hyaline, smooth, arising laterally from the hyphae, usually bearing verticils of two to four branches arising from the stipe at an acute angle (Supplementary Fig. 2D). Conidia abundant in SBA (Supplementary Fig. 2E), intercalary or terminal, gray to olive green, hyaline, verrucose; aleurioconidia obovoid to subglobose, occasionally clavate, with broad truncate basal scar, 2.6–3.7 × 1.9–2.7 µm (av = 2.98 × 2.22 µm, n = 15). Ascomata absent.

3.3. *In vivo assay against larvae of Tenebrio molitor*

Among the 11 *Pseudogymnoascus* spp. strains assessed, strains UFMGCB 8532 and UFMGCB 8562 displayed 100 % lethality within one day of contact with *T. molitor* larvae (Fig. 2), whereas the control (*C. albicans* SC5314) took 10 days to produce the same result.

3.4. *In vivo assay using BALB/c mice*

The impacts of *Pseudogymnoascus* sp. UFMGCB 8532 on the survival of immunosuppressed BALB/c mice are shown in Fig. 3A. Forty percent of infected mice succumbed after 65 d, despite no statistical difference in relation to the NI group. After infection, the animals exhibited oscillations between weight gain and loss (Fig. 3B). The presence of the fungus was analyzed in the spleen and lungs of animals, after the intranasal infection with fungal spores, with the levels detected being somewhat lower than those originally inoculated into the lung and spleen (Fig. 3C and D). There was no evidence of the presence of the fungus in the infected mouse brain tissue. In terms of function and sensory reflex (Fig. 3E), there was a significant change in scores for the infected groups after 30 d. Autonomous function (Fig. 5F), declined after 30 d of infection, followed by recovery after 40 d. The neuropsychiatric state (Fig. 3G, H, I) of infected animals showed a significant reduction

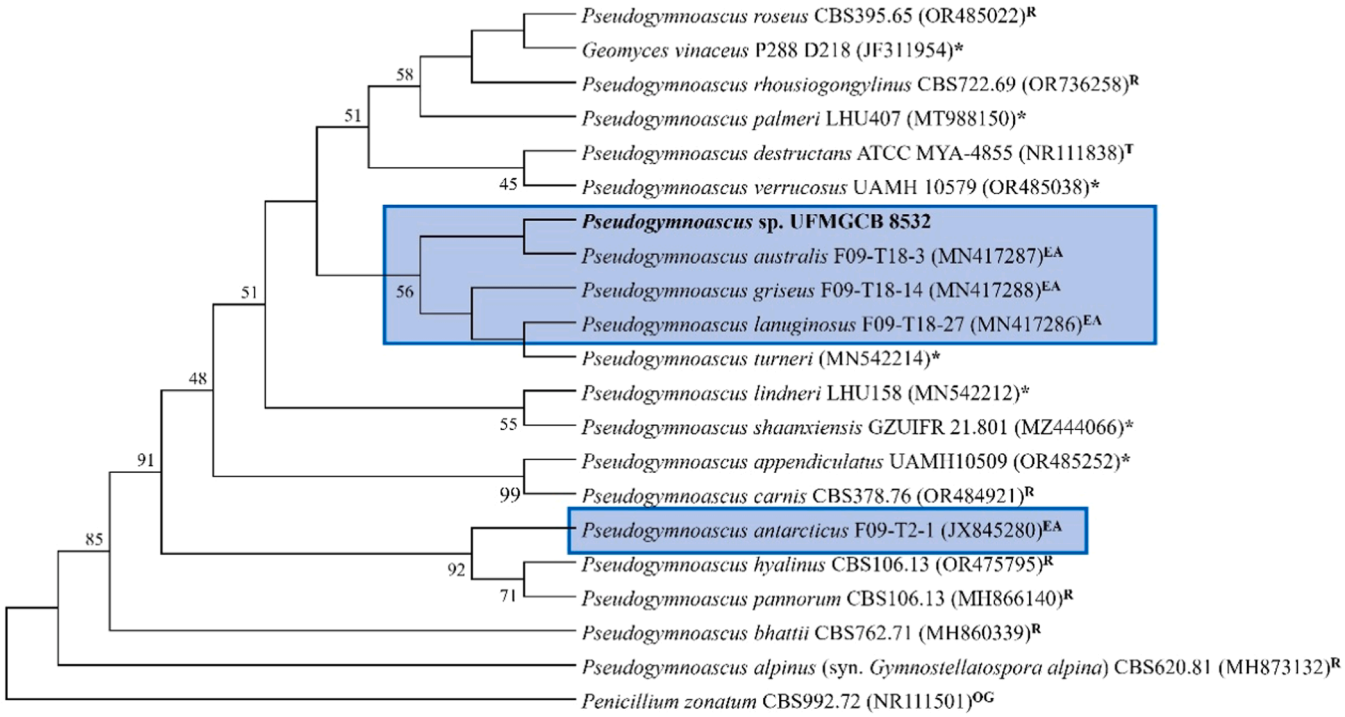

Fig. 1. Phylogenetic analysis using the ITS region including *Pseudogymnoascus* sp. UFMGCB 8532 (in bold) and other species deposited in GenBank. Blue boxes indicate taxa endemic to Antarctica. [R]Reference sequences and *Non-reference sequences deposited in GenBank, [EA]reported as endemic for Antarctica (Villanueva et al. 2021) and [OG]Outgroup. The phylogenetic tree was constructed using the maximum composite likelihood method with bootstrap values calculated from 1000 replicate runs using the program MEGA 11.

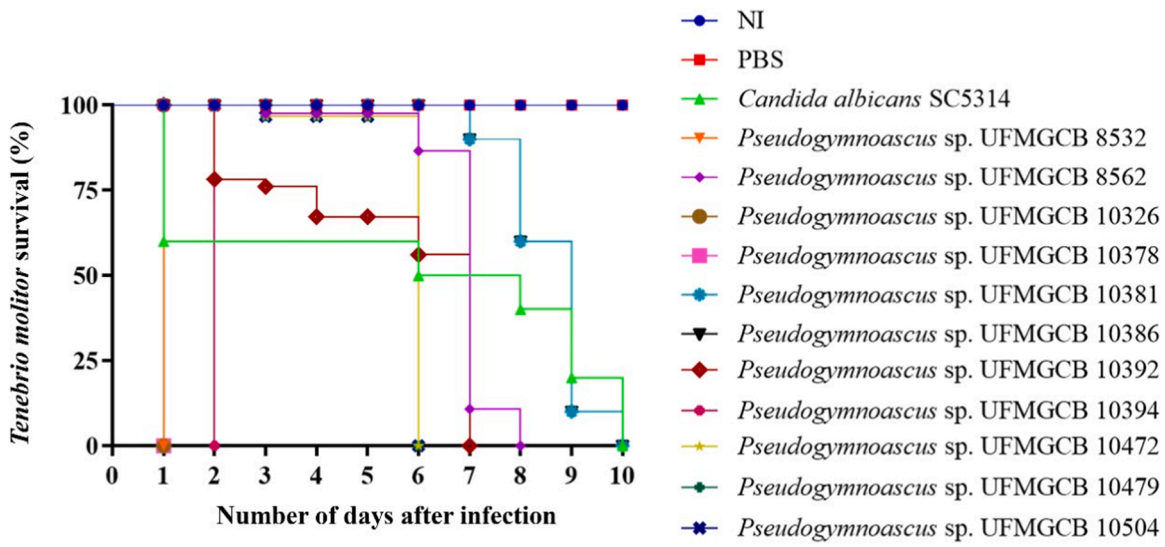

Fig. 2. Survival, expressed as percentage (%), of *Tenebrio molitor* larvae subjected to experimental infection by different *Pseudogymnoascus* spp. strains. The Log-rank test (Mantel-Cox) was used for all assays ($p < 0.0001$). NI = larva not infected and PBS = Phosphate Buffered Saline as negative control (both parameters displayed the same survive rate = 100 %).

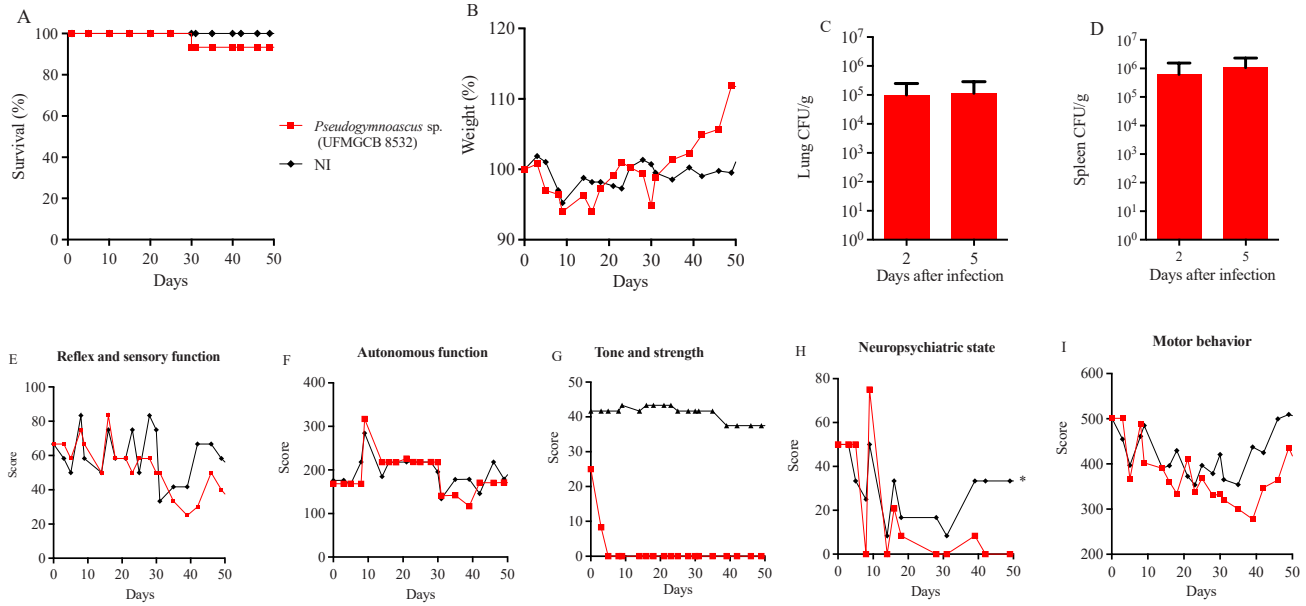

Fig. 3. Survival and behavior of immunosuppressed BALB/c mice after infection with spores of *Pseudogymnoascus* sp. UFMGCB 8532. (**A**) Survival of mice infected intranasally with 10^8 CFU (n = 6 mice per group), (**B**) weight variation over time of mice expressed as percentage (%) after infection, (**C**) fungal load recovered from the lung after 2 and 5 days of infection, (**D**) fungal load recovered from the spleen after 2 and 5 days of infection, (**E**) sensory function and reflex, (**F**) autonomous function, (**G, H**) Neuropsychiatric status and (**I**) motor behavior. (NI) Not infected. (#) In relation to NI $p<0.05$.

compared to the control group from day 18 onwards.

After recovery and quantification of the fungal load in infected mice, the recovered fungus was subjected to molecular analysis. Comparison of the electrophoretic profile of the amplified products from infected mice with those of the original inoculation indicates the same band pattern was consistently present, indicating that the inoculated fungus remained in the mice throughout the experiment (Suppl. Fig. 3).

3.5. *Histopathology of BALB/c mice infected with Pseudogymnoascus sp. UFMGCB 8532*

Histopathological examination of organs from BALB/c mice infected with *Pseudogymnoascus* sp. UFMGCB 8532 (Fig. 4) revealed that the isolate caused intense hyperemia, pulmonary edema, and an inflammatory process characterized by the presence of a large number of neutrophils and a small number of macrophages at two (Fig. 4A, B) and five (Fig. 4C, D) days post-infection. Fig. 4 shows an intense inflammatory infiltrate present primarily around the bronchioles, distributed in a multifocal to coalescent manner, composed of a large quantity of neutrophils (intact and degenerated) and a discrete number of epithelioid macrophages associated with a small number of structures measuring approximately 3 μm. These structures had a thin capsule characterized by a clear halo (normally not stained) surrounding the nucleus, which sometimes showed eosinophilic staining and was also noted in the cytoplasm of macrophages. In a few bronchioles, an inflammatory infiltrate predominantly composed of neutrophils was

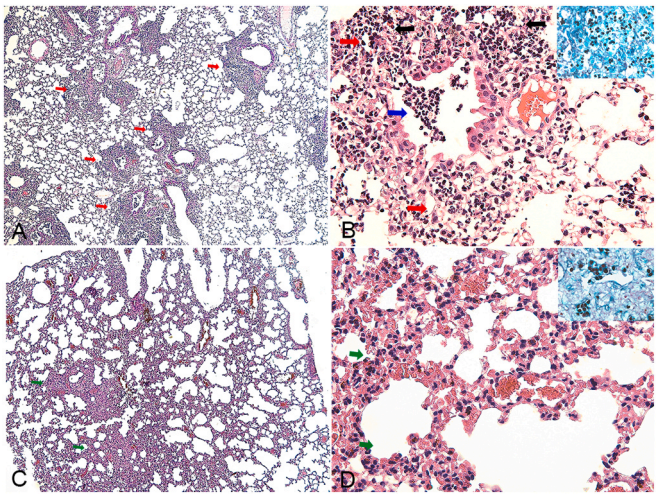

Fig. 4. Lungs of BALB/c mice two days post-intranasal infection with *Pseudogymnoascus* sp. UFMGCB 8532. (**A**) Multifocal areas of intense moderate inflammation peribronchiolar (red arrow), Hematoxylin-eosin (HE) staining, 4× objective. (**B**) Inflammatory infiltrate (red arrow) composed of many neutrophils, a discrete number of macrophages and epithelioid cells, associated with a moderate number of structures measuring approximately 3 μm, also present in the cytoplasm of macrophages (black arrow), associated with moderate hyperemia. Neutrophilic infiltrate intraluminal bronchiole (blue arrow) HE, 40× objective. In detail, the black fungal structures. Grocott's Silver Methenamine Staining 100× objective. (**C**) Animals evaluated 5 days post-infection demonstrating multifocal areas of discrete interstitial inflammatory infiltrate (green arrow). HE, objective 4×. (D) Interstitial inflammatory infiltrate (green arrow) composed of a few neutrophils and rare epithelioid macrophages, associated moderate hyperemia. HE, 40× objective. In detail, the black fungal structures. Grocott's Silver Methenamine Staining 100× objective.

present. Multifocal and discrete thickening was observed in the alveolar septa, associated with the presence of neutrophils. Additionally, moderate multifocal hyperemia and amorphous eosinophilic content within the alveoli (edema) were detected. These inflammatory changes were noted in lungs of all mice evaluated infected with *Pseudogymnoascus* sp. UFMGCB 8532. The average inflammatory score assigned for infection after two and five days, respectively, indicates that the fungus was able

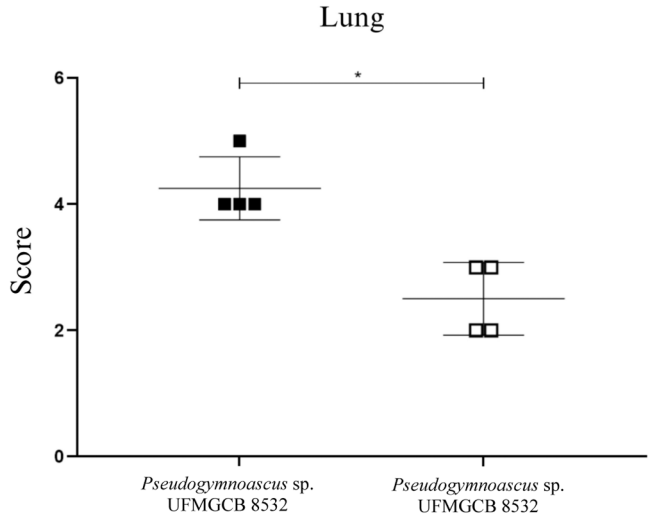

Fig. 5. Histopathological evaluation of the lungs of BALB/c mice (n = 4) intranasally infected with 1×10^8 spores and euthanized two days post-infection (black square) and five days post-infection (light square). The results were checked for normality before being analyzed using the non-parametric Mann-Whitney test (* $p < 0.05$).

to induce lung inflammation that it was higher at two days after infection (Fig. 5).

4. Discussion

4.1. In vitro pathogenicity

All isolates of *Pseudogymnoascus* spp. from Antarctica were able to grow at temperatures above 15 °C, albeit slowly at 28 °C. Gargas et al. (2009) and Verant et al. (2012) noted that the species *P. destructans*, known to be pathogenic to bats, cannot grow above 19.8 °C in *in vitro* conditions. However, other species of *Pseudogymnoascus* tolerate temperatures over 20 °C. The Antarctic strains examined in the current study, as well as the Antarctic endemic species *P. antarcticus*, *P. australis*, *P. griseus* and *P. lanuginosus*, similarly exhibit reduced growth at 25 °C suggesting they should be considered psychrotolerant, forming small pinpoint colonies (Villanueva et al., 2021).

The majority of the *Pseudogymnoascus* spp. strains tested here were able to cause partial lysis of red blood cells (α-hemolysis). According to Reynolds and Barton (2014), the α-hemolysis profile in *P. destructans* suggests that hemolytic activity occurs under nutrient limitation, a characteristic that may not be essential for the growth of the fungus in the host but may facilitate their survival by helping them obtain iron to support their growth. All tested strains were able to grow at pH 4, 7 and 9. Chaturvedi et al. (2019) similarly reported that *P. destructans* and *P. pannorum*, isolated from bats and soil in Canada, respectively, were able to grow across the same pH range, illustrating their high growth and adaptation plasticity.

According to Palmer et al. (2018), key enzymes produced by *P. destructans* can be inactivated by UV light (an abundant factor in summer in the Antarctic Peninsula), compared to other hibernacula-inhabiting fungi. However, differing from *P. destructans*, strong esterase and urease production profiles were observed for some of the Antarctic *Pseudogymnoascus* strains evaluated in our study, consistent with various previous studies of the genus (Chaturvedi et al., 2010; Fenice et al., 1997; Hayes, 2012; He et al., 2017; Holz et al., 2016; Raudabaugh and Miller, 2013; Reynolds and Barton, 2014). Ten of the strains were strong phospholipase producers, differing from Chaturvedi et al. (2010), who reported that *P. destructans* is not able to produce the enzyme.

The spore diameters of Antarctic *Pseudogymnoascus* spp. strains typically produced conidia < 4 μm, qualifying them as virulence factors of the fungus since tiny conidia with a diameter between 2 and 5 μm can reach the lung alveoli of animals (Latgé, 2001). Six strains were capable of growth under hypoxia. The mechanisms of adaptation to hypoxic conditions in fungi vary; however, some studies suggest that hypoxia is an *in vivo* stressor used by human fungal pathogens capable of directly affecting host immune responses during infection (Grahl et al., 2011; Maurer et al., 2019; Lima et al., 2015). To date, there are no reports of tests with *Pseudogymnoascus* species to verify their ability to resist hypoxic conditions. Seven strains were able to grow in 2 % NaCl conditions. According to Kochkina et al. (2007), some species of *Pseudogymnoascus*, such as *P. pannorum*, are considered halotolerant up to 10 % salt concentration (Gilichinsky et al., 2005).

Four strains exhibited resistance to the anti-fungal agent fluconazole (MIC > 64 μg mL^{-1}). Chaturvedi et al. (2011) noted that some *Pseudogymnoascus* species are susceptible to currently available antifungals, including *P. destructans*, which is sensitive to amphotericin B, itraconazole and fluconazole. Wilson et al. (2017) noted that the susceptibility *of P. destructans* to amphotericin B increased at temperatures above 15 °C, indicating that resistance mechanisms may vary with temperature.

4.2. In vivo assay against larval Tenebrio molitor

The Antarctic *Pseudogymnoascus* spp. strains caused different

mortality patterns in *T. molitor* larvae. *Pseudogymnoascus* sp. UFMGCB 8532 and UFMGCB 8562 were notably virulent, causing 100 % mortality on the first and second day, respectively. These results are similar to those reported by Beekman et al. (2018), who used *Galleria mellonella* inoculated with a concentration of 10^6 spores of *P. destructans*, and by Fuchs et al. (2018), with 10^6 spores of *P. destructans* and *P. pannorum* in *G. mellonella* larvae, resulting in reduced survival within two days.

4.3. *Pseudogymnoascus spp. strain taxonomy*

Analysis of the ITS region confirmed that all 11 strains studied were representatives of the genus *Pseudogymnoascus*. Phylogenetic comparison using the ITS region showed that the strain *Pseudogymnoascus* sp. UFMGCB 8532 was closely related to the endemic Antarctic species *P. australis*, *P. griseus*, and *P. lanuginosus*, most closely to *P. australis* as described by Villanueva et al. (2021). However, the macro- and micromorphology characteristics observed in *Pseudogymnoascus* sp. UFMGCB 8532 differed from those species. When compared to the closest species, UFMGCB 8532 showed discrepancies in colony morphology (diameter, color, presence of exudates) and micromorphology (hyphae diameter, aleuroconidia size, absence of arthroconidia), indicating that the fungus may represent a different *Pseudogymnoascus* species. Detailed taxonomic studies will be necessary to confirm the identification of *Pseudogymnoascus* sp. UFMGCB 8532.

4.4. *In vivo assay against BALB/c mice*

Different animal models, including BALB/c mice, have been used to evaluate the pathogenicity of fungi (Conti et al., 2014). *Pseudogymnoascus* sp. UFMGCB 8532 was selected for this part of the study because it exhibited relevant virulence and stress tolerance factors *in vitro* and showed the most rapid activity against *T. molitor* larvae. In addition, differences in survival or behavior of immunocompromised mice were observed. Changes in the neuropsychiatric state were also evident, suggesting encephalopathy (disruption of brain function) (Jeremias, 2015). The fungus was recovered from the spleen and lung of infected mice, but not from brain tissue. This is the first study to use BALB/c mice as an animal model to study the pathogenicity of *Pseudogymnoascus*.

4.5. *Inflammation induced by Pseudogymnoascus sp. UFMGCB 8532 in lungs of BALB/c mice*

We showed intranasal infection with *Pseudogymnoascus* sp. UFMGCB 8532 could induce an acute inflammatory response in mice lungs, characterized by hyperemia, edema and neutrophil and macrophage infiltration. The lung inflammation reduced from second to fifth day of infection. Despite the lack of information about the inflammatory processes caused by Antarctic *Pseudogymnoascus* species, previous studies have shown that different *P. destructans* strains have the potential to cause inflammation in infected tissues. According to Pikula et al. (2017), erosion of bat wings is caused by inflammation due to the presence of fungi in their skin. In addition, Field et al. (2015) showed that the bat species *Myotis lucifugus* from North America, when infected with *P. destructans*, expresses genes associated with local inflammation in the skin. In summary, *P. destructans* causes important disease in bats with skin inflammation associated with fungal hyphae (Meteyer et al., 2009; 2012; Kacprzyk et al. 2017; Pikula et al., 2017; Isidoro-Ayza and Klein, 2024). Bats infected with *P. destructans* experience an initially slow inflammatory process that drastically accelerates as hibernation progresses (Pikula et al., 2017; Fritze et al., 2019).

5. Conclusions

The data obtained in this study indicate that various *Pseudogymnoascus* spp. strains, obtained from different substrates/habitats in maritime Antarctica, may show features of potential virulence towards experimental animal hosts, particularly those that are already immunocompromised. Given that the Antarctic environment is an important reservoir for *Pseudogymnoascus* species, which display growth across a range of temperatures, it is possible that increasing temperatures in the maritime Antarctic due to climate change could activate dormant genes or biochemical pathways, select virulent species and/or strains, and facilitate their spread within and beyond the region. The ability of *Pseudogymnoascus* species to grow slowly even at 28°C, coupled with their potential *in vitro* and *in vivo* virulence factors, suggests that these fungi might be undergoing an opportunistic transition due to the effects of climate change on the Antarctic Peninsula. Our results reinforce the need for greater understanding of the biochemical and potentially pathogenic capabilities of opportunistic microorganisms present in Antarctica and other cold regions globally.

CRediT authorship contribution statement

Vívian Gonçalves: Writing – original draft, Methodology, Formal analysis, Conceptualization. **Marliete Costa:** Writing – original draft, Methodology, Investigation, Formal analysis, Conceptualization. **Eldon Gomes:** Writing – original draft, Methodology, Data curation, Conceptualization. **Gustavo Freitas:** Writing – original draft, Methodology, Investigation, Formal analysis. **Daniel Santo:** Writing – original draft, Methodology, Formal analysis. **Susana Johann:** Writing – original draft, Methodology, Formal analysis, Conceptualization. **Peter Convey:** Writing – review & editing, Writing – original draft, Validation, Methodology, Conceptualization. **Luiz Rosa:** Writing – review & editing, Writing – original draft, Supervision, Methodology, Investigation, Funding acquisition, Formal analysis, Conceptualization. **Jefferson Oliveira:** Writing – original draft, Methodology, Investigation, Formal analysis. **Tatiane Paixão:** Writing – original draft, Methodology, Investigation, Formal analysis.

Declaration of Competing Interest

The authors have no competing interest to declare that are relevant to the content of this article.

Acknowledgements

This study received financial support from CNPq, CAPES, FNDCT, FAPEMIG, INCT Criosfera, PROANTAR and Brazilian Navy. P. Convey is supported by NERC core funding to the British Antarctic Survey's 'Biodiversity Evolution and Adaptation' Team.

Appendix A. Supporting information

Supplementary data associated with this article can be found in the online version at doi:10.1016/j.microb.2024.100186.

Data Availability

Data will be made available on request.

References

Altschul, S.F., Madden, T.L., Schafer, A.A., Zhang, J.H., Zhang, Z., Miller, W., Lipman, D. J., 1997. Gapped BLAST and PSI-BLAST: a new generation of protein database search programs. Nucleic Acids Res. 25, 3389–3402. https://doi.org/10.1093/nar/25.17.3389.

Alves, I.M., Gonçalves, V.N., Oliveira, F.S., Schaefer, C.E., Rosa, C.A., Rosa, L.H., 2019. The diversity. distribution. and pathogenic potential of cultivable fungi present in rocks from the South Shetlands archipelago, Maritime Antarctica. Extremophiles 23, 327–336. https://doi.org/10.1007/s00792-019-01086-8.

Aoki, S., Ito-Kuwa, S., Nakamura, Y., Masuhara, T., 1990. Comparative pathogenicity of wild-type strains and respiratory mutants of *Candida albicans* in mice. Zent. Bakteriol. 273, 332–343. https://doi.org/10.1016/S0934-8840(11)80437-8.

Arenz, B.E., Blanchette, R.A., 2011. Distribution and abundance of soil fungi in Antarctica at sites on the Peninsula, Ross Sea Region and McMurdo Dry Valleys. Blanchette 43, 308–315. https://doi.org/10.1016/j.soilbio.2010.10.016.

Arenz, B.E., Blanchette, R.A., Farrell, R.L., 2014. Fungal diversity in Antarctic soils. In: Cowan, D. (Ed.), Antarctic terrestrial microbiology: physical and biological properties of Antarctic soils. Springer, Berlin, Heidelberg, pp. 35–53. https://doi.org/10.1007/978-3-642-45213-0_3.

Beekman, C.N., Meckler, L., Kim, E., Bennett, R.J., 2018. *Galleria mellonella* as an insect model for *P. destructans*, the cause of White-nose Syndrome in bats. Plos One 13, e0201915. https://doi.org/10.1371/journal.pone.0201915.

Blehert, D.S., 2012. Fungal disease and the developing story of bat White-nose Syndrome. PLoS. Pathog. 8, e1002779. https://doi.org/10.1371/journal.ppat.1002779.

Blehert, D.S., Hicks, A.C., Behr, M.J., Meteyer, C.U., Berlowski-Zier, B.M., Buckles, E.L., Coleman, J.T.H., Darling, S.R., Gargas, A., Niver, R., Okoniewski, J.C., Rudd, R.J., Stone, W.B., 2009. Bat white-nose syndrome: an emerging fungal pathogen?, 227 Science 323, 227. https://doi.org/10.1126/science.1163874.

Brunati, M., Rojas, J.L., Sponga, F., Ciciliato, I., Losi, D., Göttlich, E., De Hoog, S., Genilloud, O., Marinelli, F., 2009. Diversity and pharmaceutical screening of fungi from benthic mats of Antarctic lakes. Mar. Genom. 2, 43–50. https://doi.org/10.1016/j.margen.2009.04.002.

Casadevall, A., 2012. Fungi and the rise of mammals. PLoS Pathog. 8, e1002808. https://doi.org/10.1371/journal.ppat.1002808.

Chaturvedi, V., Defiglio, H., Chaturvedi, S., 2019. Phenotype profiling of white nose syndrome pathogen *Pseudogymnoascus destructans* and closely-related *Pseudogymnoascus pannorum* reveals metabolic differences underlying fungal lifestyles. F1000Research 7, 665. https://doi.org/10.12688/f1000research.15067.2.

Chaturvedi, S., Rajkumar, S.S., Li, X., Hurteau, G.J., Shutman, M., Chaturvedi, V., 2011. Antifungal testing and high-throughput screening of compound library against *Geomyces destructans*, the etiologic agent of geomycosis (WNS) in bats. PLoS One 6, e17032. https://doi.org/10.1371/journal.pone.0017032.

Chaturvedi, V., Springer, D.J., Behr, M., 2010. Morphological and molecular characterizations of psychrophilic fungus *Geomyces destructans* from New York bats with White Nose Syndrome (WNS). PLoS One 5, e10783. https://doi.org/10.1371/journal.pone.0010783.

Chávez, R., Fierro, F., García-Rico, R., 2015. Filamentous fungi from extreme environments as a promising source of novel bioactive secondary metabolites. Front. Microbiol. 6, 903. https://doi.org/10.3389/fmicb.2015.00903.

Christensen, W.B., 1946. Urea decomposition as a means of differentiating *Proteus* and paracolon cultures from each other and from *Salmonella* and *Shigella* Types. J. Bacteriol. 52, 461–466.

CLSI (2008) Reference method for broth dilution antifungal susceptibility testing of filamentous fungi; approved standard CLSI document M38-A2. Clinical and Laboratory Standards 30 Institute, Wayne.

Connell, L., Segee, B., Redman, R., Rodriguez, R.J., Staudige, H., 2018. Biodiversity and abundance of cultured microfungi from the permanently ice-covered Lake Fryxell, Antarctica. Life 8, 1–10. https://doi.org/10.3390/life8030037.

Conti, H.R., Huppler, A.R., Whibley, N., Gaffen, S.L., 2014. Animal models for candidiasis, 6.17 Curr. Protoc. Immunol. 105 (19.6), 1–19. https://doi.org/10.1002/0471142735.im1906s105.

Costa, M.C., Santos, J.R.A., Ribeiro, M.J.A., De Freitas, G.J.C., Bastos, R.W., Ferreira, G. F., Miranda, A.S., Nascimento, R.D., Santos, A.P.C., Martins, F.S., Paixão, T.A., Teixeira, A.L., Souza, D.G., Santos, D.A., 2016. The absence of microbiota delays the inflammatory response to *Cryptococcus gattii*. J. Med. Microbiol. 306, 187–195. https://doi.org/10.1016/j.ijmm.2016.03.010.

Cunha, M.M., Franznen, A.J., Seabra, S.H., Herbst, M.H.H., Vugman, N.V., Borba, L.P., Souza, W., Rozental, S., 2010. Melanin in *Fonsecaea pedrosoi*: a trap for oxidative radicals. BMC Microbiol 10, 80. https://doi.org/10.1186/1471-2180-10-80.

Davis, D.A., 2009. How human pathogenic fungi sense and adapt to pH: the link to virulence. Curr. Opin. Microbiol. 12, 365–370. https://doi.org/10.1016/j.mib.2009.05.006.

Edgington, S., Thompson, E., Moore, D., Hughes, K.A., Bridge, P., 2014. Investigating the insecticidal potential of *Geomyces* (Myxotrichaceae: Helotiales) and *Mortierella* (Mortierellacea: Mortierellales) isolated from Antarctica. Springerplus 3, 289. https://doi.org/10.1186/2193-1801-3-289.

Evans, S., Hansen, R.W., Schneegurt, M.A., 2013. Isolation and characterization of halotolerant soil fungi from the great salt plains of Oklahoma. Cryptogam. Mycol. 34, 329–341. https://doi.org/10.7872/crym.v34.iss4.2013.329.

Fenice, M., Selbmann, L., Zucconi, L., Onofri, S., 1997. Production of extracellular enzymes by Antarctic fungal strains. Polar Biol. 17, 275–280. https://doi.org/10.1007/s003000050132.

Ferreira, G.F., Santos, J.R., Costa, M.C., Holanda, R.A., Denadai, A.M., Freitas, G.J., Santos, A.R., Tavares, P.B., Paixão, T.A., Santos, D.A., 2015. Heteroresistance to itraconazole alters the morphology and increases the virulence of *Cryptococcus gattii*. Antimicrob. Agents Chemother. 59, 4600–4609 https://doi.org/10.1128/AAC.00466-15.

Field, K.A., Johnson, J.S., Lilley, T.M., Reeder, S.M., Rogers, E.J., Behr, M.J., et al., 2015. The white-nose syndrome transcriptome: activation of anti-fungal host responses in wing tissue of hibernating little brown myotis. PloS Pathog. 11, e1005168. https://doi.org/10.1371/journal.ppat.1005168.

Figueredo, H.M., Gonçalves, V.N., Godinho, V.M., Lopes, D.V., Oliveira, F.S., Rosa, L.H., 2020. Diversity and ecology of cultivable fungi isolated from the thermal soil gradients in Deception Island, Antarctica. Extremophiles 24, 219–225. https://doi.org/10.1007/s00792-019-01146-z.

Figueroa, L., Jiménez, C., Rodríguez, J., 2015. 3-Nitroasterric acid derivatives from an Antarctic sponge-derived *Pseudogymnoascus* sp. fungus. J. Nat. Prod. 78, 919–923. https://doi.org/10.1021/np500906k.

Fisher, M.C., Henk, D.A., Briggs, C.J., Brownstein, J.S., Madoff, L.C., Mccraw, S.L., Gurr, S.J., 2012. Emerging fungal threats to animal, plant and ecosystem health. Nature 484, 186–194. https://doi.org/10.1038/nature10947.

Fritze, M., Costantini, D., Fickel, J., Wehner, D., Czirják, G.Á., Voigt, C.C., 2019. Immune response of hibernating European bats to a fungal challenge. bio046078 Biol. Open 8. https://doi.org/10.1242/bio.046078.

Fuchs, B.B., Chaturvedi, S., Rossoni, R.D., Barros, P.P., Torres-Velez, F., Mylonakis, E., Chaturvedi, V., 2018. *Galleria mellonella* experimental model for bat fungal pathogen *Pseudogymnoascus destructans* and human fungal pathogen *Pseudogymnoascus pannorum*. Virulence 9, 1539–1547. https://doi.org/10.1080/21505594.2018.1518087.

Furbino, L.E., Godinho, V.M., Santiago, I.F., Pellizari, F.M., Alves, T.M., Zani, C.L., Junior, A.S.P., Romanha, A.J., Carvalho, A.G.O., Gil, L.H.V.G., Rosa, C.A., Minnis, A. M., Rosa, L.H., 2014. Diversity patterns, ecology and biological activities of fungal communities associated with the endemic macroalgae across the Antarctic Peninsula. Microb. Ecol. 67, 775–787. https://doi.org/10.1007/s00248-014-0374-9.

Gargas, A., Trest, M.T., Christensen, M., Volk, T.J., Blehert, D.S., 2009. *Geomyces destructans* sp. nov. associated with bat white-nose syndrome. Mycotaxon 108, 147–154. https://doi.org/10.5248/108.147.

Gilichinsky, D., Rivkina, E., Bakermans, C., Shcherbakova, V., Petrovskaya, L., Ozerskaya, S., Ivanushkina, N., Kochkina, G., Laurinavichuis, K., Pecheritsina, S., Fattakhova, R., Tiedje, J.M., 2005. Biodiversity of cryopegs in permafrost. Microb. Ecol. 53, 117–128. https://doi.org/10.1016/j.femsec.2005.02.003.

Godinho, V.M., Gonçalves, V.N., Santiago, I.F., Figueredo, H.M., Vitoreli, G.A., Schaefer, C.E.G.R., Barbosa, E.C., Oliveira, J.G., Alves, T.M.A., Zani, C.L., Junior, P. A.S., Murta, S.M.F., Romanha, A.J., Kroon, E.G., Cantrell, C.L., Wedge, D.E., Duke, S. O., Ali, A., Rosa, C.A., Rosa, L.H., 2015. Diversity and bioprospection of fungal community present in oligotrophic soil of continental Antarctica. Extremophiles 19, 585–596. https://doi.org/10.1007/s00792-015-0741-6.

Gonçalves, V.N., Carvalho, C.R., Johann, S., Mendes, G., Alves, T.M., Zani, C.L., Junior, P.A.S., Murta, S.M.F., Romanha, A.J., Cantrell, C.L., Rosa, C.A., Rosa, L.H., 2015. Antibacterial, antifungal and antiprotozoal activities of fungal communities present in different substrates from Antarctica. Polar Biol. 38, 1143–1152. https://doi.org/10.1007/s00300-015-1672-5.

Gonçalves, V.N., Oliveira, F.S., Carvalho, C.R., Schaefer, C.E.G.R., Rosa, C.A., Rosa, L.H., 2017. Antarctic rocks from continental Antarctica as source of potential human opportunistic fungi. Extremophiles 21, 851–860. https://doi.org/10.1007/s00792-017-0947-x.

Grahl, N., Puttikamonkul, S., Macdonald, J.M., Gamcsik, M.P., Ngo, L.Y., Hohl, T.M., Cramer, R.A., 2011. *In vivo* hypoxia and a fungal alcohol dehydrogenase influence the pathogenesis of invasive pulmonary aspergillosis. PLOS Pathog. 7, e1002145. https://doi.org/10.1371/journal.ppat.1002145.

Hayes, M.A., 2012. The *Geomyces* fungi: ecology and distribution. BioScience 62, 819–823. https://doi.org/10.1525/bio.2012.62.9.7.

He, L., Mao, Y., Zhang, L., Wang, H., Alias, S.A., Gao, B., Wei, D., 2017. Functional expression of a novel α-amylase from Antarctic psychrotolerant fungus for baking industry and its magnetic immobilization. BMC Biotechnol. 17, 22. https://doi.org/10.1186/s12896-017-0343-8.

Holz, P., Hufschmid, J., Boardman, W., Cassey, P., Firestone, S., Lumsden, L., Prowse, T., Reardon, T., Stevenson, M., 2016. Qualitative risk assessment: White-nose syndrome in bats in Australia. Qualitative risk assessment: White-nose syndrome in bats in Australia. Wildlife Health Australia, Sydney, NSW, Australia.

Hoyt, J.R., Cheng, T.L., Langwig, K.E., Hee, M.M., Frick, W.F., Kilpatrick, A.M., 2015. Bacteria isolated from bats inhibit the growth of *Pseudogymnoascus destructans*, the causative agent of White-Nose Syndrome. PLOS One 10, e0121329. https://doi.org/10.1371/journal.pone.0121329.

Isidoro-Ayza, M., Klein, B.S., 2024. Pathogenic strategies of *Pseudogymnoascus destructans* during torpor and arousal of hibernating bats. Science 385, 194–200. https://doi.org/10.1126/science.adn5606.

Jeremias, I.C., 2015. Investigação das alterações imunológicas em camundongos submetidos ao modelo animal de sepse por ligação e perfuração cecal (CLP) com alterações cerebrais. ⟨https://www.teses.usp.br/teses/disponiveis/5/5165/tde-06112015-143205/publico/IsabelaCasagrandeJeremias.pdf⟩. https://doi.org/10.11606/T.5.2015.tde-06112015-143205. (accessed17 January 2024).

Kacprzyk, J., Hughes, G.M., Palsson-Mcdermott, E.M., Quinn, S.R., Puechmaille, S.J., O'neill, L.A.J., et al., 2017. A potent anti-inflammatory response in bat macrophages may be linked to extended longevity and viral tolerance. Acta Chiropterol 19, 219–228.

Lackner, P., Beer, R., Heussler, V., Goebel, G., Rudzki, D., Helbok, R., Tannich, E., Schmutzhard, E., 2006. Behavioural and histopathological alterations in mice with cerebral malaria. Neuropathol. Appl. Neurobiol. 32, 177–188. https://doi.org/10.1111/j.1365-2990.2006.00706.x.

Latge, J.P., 2001. The pathobiology of *Aspergillus fumigatus*. Trends Microbiol 9, 382–389. https://doi.org/10.1016/S0966-842X(01)02104-7.

Li, Y., Sun, B., Liu, S., 2008. Bioactive asterric acid derivatives from the Antarctic ascomycete fungus *Geomyces* sp. J. Nat. Prod. 71, 1643–1646. https://doi.org/10.1021/np8003003.

Lima, P.S., Chung, D., Bailão, A.M., Cramer, R.A., Soares, C.M.A., 2015. Characterization of the *Paracoccidioides* hypoxia response reveals new insights into pathogenesis mechanisms of this important human pathogenic fungus. PLoS Negl. Trop. Dis. 9, e0004282. https://doi.org/10.1371/journal.pntd.0004282.

Lorch, J.M., Meteyer, C.U., Behr, M.J., Boyles, J.G., Cryan, P.M., Hicks, A.C., Ballmann, A., Coleman, J.T.H., Redell, D.N., Reeder, D., Blehert, D.S., 2011.

Experimental infection of bats with *Geomyces destructans* causes white-nose syndrome. Nature 480, 376–378. https://doi.org/10.1038/nature10590.
Martorell, M.M., Ruberto, L.A.M., Fernández, P.M., Castellanos de Figueroa, L.I., Mac Cormack, W.P., 2017. Bioprospection of cold-adapted yeasts with biotechnological potential from Antarctica. J. B. Microbiol. 57, 504–516. https://doi.org/10.1002/jobm.201700021.
Maurer, E., Aigner, M., Lass-Flörl, C., Binder, U., 2019. Hypoxia decreases diagnostic biomarkers for *Aspergillosis in vitro*. J. Fungi. 5, 61. https://doi.org/10.3390/jof5030061.
Mercantini, R., Marsellam, R., Cervellati, C., 1989. Keratinophilic fungi isolated from antarctic soil. Mycopathologia 106, 47–52. https://doi.org/10.1007/BF00436926.
Meteyer, C.U., Barber, D., Mandl, J.N., 2012. Pathology in euthermic bats with white nose syndrome suggests a natural manifestation of immune reconstitution inflammatory syndrome. Virulence 3, 583–588. https://doi.org/10.4161/viru.22330.
Meteyer, C.U., Buckles, E.L., Blehert, D.S., Hicks, A.C., Green, D.E., Shearn-Bochsler, V. E., Thomas, N.J., Gargas, A., Behr, M.J., 2009. Histopathologic criteria to confirm white-nose syndrome in bats. J. Vet. Diagn. Invest. 21, 411–414. https://doi.org/10.1177/104063870902100401.
Oliveira, L.V.N., Costa, M.C., Magalhães, T.F.F., Bastos, R.W., Santos, P.C., Carneiro, H.C. S., Ribeiro, N.Q., Ferreira, G.F., Ribeiro, L.S., Gonçalves, A.P.F., Fagundes, C.T., Pascoal-Xavier, M.A., Djordjevic, J.T., Sorrell, T.C., Souza, D.G., Machado, A.M.V., Santos, D.A., 2017. Influenza A virus as a predisposing factor for cryptococcosis. Front. Cell. Infect. Microbiol. 7, 419. https://doi.org/10.3389/fcimb.2017.00419.
Onofri, S., 1999. Antarctic Microfungi. In: Seckbach, J. (Ed.), Enigmatic Microorganisms and Life in Extreme Environments. Cellular Origin and Life in Extreme Habitats. Springer, Dordrecht, pp. 323–336. https://doi.org/10.1007/978-94-011-4838-2_26.
Palmer, J.M., Drees, K.P., Foster, J.T., Lindner, D.L., 2018. Extreme sensitivity to ultraviolet light in the fungal pathogen causing white-nose syndrome of bats. Nat. Commun. 9, 35. https://doi.org/10.1038/s41467-017-02441-z.
Parrish, N.M., Riedel, S., 2014. Microbiology Tools for the Epidemiologist. In: Nelson, K. E., Williams, C.M. (Eds.), Infectious disease epidemiology: theory and practice. Jones & Bartlett Learning, Burlington, USA, pp. 198–204.
Pedroso, V.S.P., Vilela, M.C., Santos, P.C., Cisalpino, O.S., Arantes, R.M.E., Rachid, M.A., Teixeira, A.L., 2010. Development of a murine model of neuroparacoccidioidomycosis. J. Neuroparasitology. 1, 39–44. https://doi.org/10.4303/jnp/N100402.
Pikula, J., Amelon, S.K., Bandouchova, H., Bartonička, T., Berkova, H., Brichta, J., Hooper, S., Kokurewicz, T., Kolarik, M., Köllner, B., Kovacova, V., Linhart, P., Piacek, V., Turner, G.G., Zukal, J., Martínková, N., 2017. White-nose syndrome pathology grading in Nearctic and Palearctic bats. PLOS One 12, e0180435. https://doi.org/10.1371/journal.pone.0180435.
Price, M.F., Wilkinson, L.D., Gentry, L.O., 1982. Plate method for detection of phospholipase activity in *Candida albicans*. Sabouraud 20, 7–14. https://doi.org/10.1080/00362178285380031.
Purić, J., Vieira, G., Cavalca, L.B., 2018. Activity of Antarctic fungi extracts against phytopathogenic bacteria. Lett. Appl. Microbiol. 66, 530–536. https://doi.org/10.1111/lam.12875.
Raudabaugh, D.B., Miller, A.N., 2013. Nutritional capability of and substrate suitability for *Pseudogymnoascus destructans*, the causal agent of bat white-nose syndrome. PLoS One 10, e78300. https://doi.org/10.1371/journal.pone.0078300.
Reynolds, H.T., Barton, H.A., 2014. Comparison of the white-nose syndrome agent *Pseudogymnoascus destructans* to cave-dwelling relatives suggests reduced saprotrophic enzyme activity. PLoS One 9, e86437. https://doi.org/10.1371/journal.pone.0086437.
Rosa, L.H., de Sousa, J.R.P., de Menezes, G.C.A., da Costa Coelho, L., Carvalho-Silva, M., Convey, P., Câmara, P.E.A.S., 2020. Opportunistic fungal assemblages present on fairy rings spread on different moss species in the Antarctic Peninsula. Polar Biol. 43, 587–596. https://doi.org/10.1007/s00300-020-02663-w.
Rosa, L.H., Vaz, A.B.M., Caligiorne, R.B., Campolina, S., Rosa, C.A., 2009. Endophytic fungi associated with the Antarctic Grass *Deschampsia antarctica* Desv. (*Poaceae*). Polar Biol. 32, 161–167. https://doi.org/10.1007/s00300-008-0515-z.
Rosa, L.H., Zani, C.L., Cantrell, C.L., Duke, S.O., Van Dijck, P., Desideri, A., Rosa, C.A., 2019. Fungi in Antarctica: diversity, ecology, effects of climate change and bioprospection for bioactive compounds. In: Rosa, L.H. (Ed.), Fungi of Antarctica: diversity, ecology and biotechnological applications. Springer, Berlin, pp. 1–17. https://doi.org/10.1007/978-3-030-18367-7_1.
Ruisi, S., Barreca, D., Selbmann, L., Zucconi, L., Onofri, S., 2007. Fungi in Antarctica. Rev. Environ. Sci. Biotechnol. 6, 127–141. https://doi.org/10.1007/s11157-006-9107-y.
Santiago, I.F., Soares, M.A., Rosa, C.H., Rosa, L.H., 2015. Lichensphere: a protected natural microhabitat of the non-lichenised fungal communities living in extreme environments of Antarctica. Extremophiles 19, 1087–1097. https://doi.org/10.1007/s00792-015-0781-y.
Santiago-Tirado, F.H., Klein, R.S., Doering, T.L., 2019. An *In vitro* brain endothelial model for studies of cryptococcal transmigration into the central nervous system. Curr. Protoc. Microbiol. 53, e78. https://doi.org/10.1002/cpmc.78.
Santos, D.A., Hamdan, J.S., 2005. Evaluation of broth microdilution antifungal susceptibility testing conditions for *Trichophyton rubrum*. J. Clin. Mic. 43, 1917–1920. https://doi.org/10.1128/jcm.43.4.1917-1920.2005.
Santos, J.R., Holanda, R.A., Frases, S., Bravim, M., Araujo, G.S., Santos, P.C., Costa, M.C., Ribeiro, M.J.A., Ferreira, G.F., Baltazar, L.M., Miranda, A.S., Oliveira, D.B., Santos, C.M.A., Fontes, A.C.L., Gouveia, L.F., Resende-Stoianoff, M.A., Abrahão, J.S., Teixeira, A.L., Paixão, T.A., Souza, D.G., Santos, D.A., 2014. Fluconazole alters the polysaccharide capsule of *Cryptococcus gattii* and leads to distinct behaviors in murine Cryptococcosis. PLoS One 19, e112669. https://doi.org/10.1371/journal.pone.0112669.
dos Santos Brito, M.M., da Silva Lima, M., Morgado, F.N., Raibolt, P., Menezes, R., Conceição-Silva, F., de Moraes Borba, C., 2011. Characteristics of *Paecilomyces lilacinus* infection comparing immunocompetent with immunosuppressed murine model. Mycoses 54, e513–e521. https://doi.org/10.1111/j.1439-0507.2010.01969.x.
Schaufuss, P., Muller, F., Valentin-Weigand, P., 2007. Isolation and characterization of a haemolysin from *Trichophyton mentagrophytes*. Vet. Microbiol. 122, 342–349. https://doi.org/10.1016/j.vetmic.2007.01.022.
Silva, A.P.R., Valerio, A.D., Viana, R.O., Ricoy, A.C.D.S., Johann, S., Alves, V.D.S., 2018. *Caenorhabditis elegans* and *Tenebrio molitor* - new tools to investigate *Malassezia* species, 2018100001. Preprints https://doi.org/10.20944/preprints201810.0001.v1.
de Sousa, J.R., Goncalves, V.N., de Holanda, R.A., Santos, D.A., Bueloni, C.F., Costa, A. O., Petry, M.V., Rosa, C.A., Rosa, L.H., 2017. Pathogenic potential of environmental resident fungi from ornithogenic soils of Antarctica. Fungal Biol. 121, 991–1000. https://doi.org/10.1016/j.funbio.2017.09.005.
Tamura, K., Stecher, G., Kumar, S., 2021. MEGA11: molecular evolutionary genetics analysis version 11. Mol. Biol. Evol. 38, 3022–3027. https://doi.org/10.1093/molbev/msab120.
Tsuji, M., Fujiu, S., Xião, N., Hanada, Y., Kudosh, S., Kondo, H., Tsuda, S., Hoshino, T., 2013. Cold adaptation of fungi obtained from soil and lake sediment in the Skarvsnes ice-free area, Antarctica. FEMS Microbiol. Lett. 346, 121–130. https://doi.org/10.1111/1574-6968.12217.
Verant, M.L., Boyles, J.G., Waldrep, W.J., 2012. Temperature-dependent growth of *Geomyces destructans*, the fungus that causes bat white-nose syndrome. PLoS One 7, e46280. https://doi.org/10.1371/journal.pone.0046280.
Villanueva, P., Vásquez, G., Gil-Durán, C., Oliva, V., Díaz, A., Henríquez, M., Álvarez, E., Laich, F., Chávez, R., Vaca, I., 2021. Description of the first four species of the genus *Pseudogymnoascus* from Antarctica. Front. Microbiol. 12, 713189. https://doi.org/10.3389/fmicb.2021.713189.
White, T.J., Bruns, T., Lee, S.J.W.T., Taylor, J., 1990. Amplification and direct sequencing of fungal ribosomal RNA genes for phylogenetics. In: Innis, M.A., Gelfand, D.H., Sninsky, J.J., White, T.J. (Eds.), PCR Protocols: a Guide to Methods and Applications. Academic Press, San Diego, pp. 315–322.
Wilson, M.B., Held, B.W., Freiborg, A.H., Blanchette, R.A., Salomon, C.E., 2017. Resource capture and competitive ability of non-pathogenic *Pseudogymnoascus* spp. and *P. destructans*, the cause of white-nose syndrome in bats. PLoS One 12, e0178968. https://doi.org/10.1371/journal.pone.0178968.
Zukal, J., Bandouchova, H., Brichta, J., Cmokova, A., Jaron, K.S., Kolarik, M., Kovacova, V., Kubátová, A., Orlov, O., Pikula, J., Presetnik, P., Šuba, J., Zahrdníková, A.J., Martínková, N., 2016. White-nose syndrome without borders: *Pseudogymnoascus destructans* infection tolerated in Europe and Palearctic Asia but not in North America. Sci. Rep. 6, 19829. https://doi.org/10.1038/srep19829.